Indian J Microbiol (Apr–June 2014) 54(2):196–202
DOI 10.1007/s12088-013-0437-5

ORIGINAL ARTICLE

# Synthesis of Silver and Gold Nanoparticles Using Cashew Nut Shell Liquid and Its Antibacterial Activity Against Fish Pathogens

**Palanivel Velmurugan · Mahudunan Iydroose · Sang-Myung Lee · Min Cho · Jung-Hee Park · Vellingiri Balachandar · Byung-Taek Oh**

Received: 25 June 2013 / Accepted: 21 October 2013 / Published online: 14 November 2013


**Abstract** This study reveals a green process for the production of multi-morphological silver (Ag NPs) and gold (Au NPs) nanoparticles, synthesized using an agro-industrial residue cashew nut shell liquid. Aqueous solutions of $Ag^{+}$ ions for silver and chloroaurate ions for gold were treated with cashew nut shell extract for the formation of Ag and Au NPs. The nano metallic dispersions were characterized by measuring the surface plasmon absorbance at 440 and 546 nm for Ag and Au NPs. Transmission electron microscopy showed the formation of nanoparticles in the range of 5–20 nm for silver and gold with assorted morphologies such as round, triangular, spherical and irregular. Scanning electron microscopy with energy dispersive spectroscopy and X-ray diffraction analyses of the freeze-dried powder confirmed the formation of metallic Ag and Au NPs in crystalline form. Further analysis by Fourier transform infrared spectroscopy provided evidence for the presence of various biomolecules, which might be responsible for the reduction of silver and gold ions. The obtained Ag and Au NPs had significant antibacterial activity, minimum inhibitory concentration and minimum bactericidal concentration on bacteria associated with fish diseases.

**Keywords** Antibacterial activity · Cashew nut shell liquid · Fish pathogens · Gold · Silver · Nanoparticles

## Introduction

The creation of nanoscale materials for advanced structures has led to a growing interest in the area of biomineralization. The cashew tree, *Anacardium occidentale* L. is a botanical species native to eastern Brazil that was introduced into other tropical countries such as India, Africa, Indonesia and South East Asia in the 16th century [1, 2]. The true fruit of a cashew is the nut, a kidney-shaped structure approximately 2–3 cm in length, which is attached to the end of a fleshy bulb, generally called the cashew apple. The shell comprises 50 % of the weight of the raw nut, the kernel represents 25 % and the remaining 25 % consists of the natural cashew nut shell liquid (CNSL), a viscous reddish brown liquid [2]. Crude CNSL represents one of the major and cheapest sources of naturally occurring non-isoprenoid phenolic lipids, including anacardic acids, cardols, cardanols, methylcardols, and polymeric materials, this might be also responsible for the production of nanoparticles [3]. CNSL has found important commercial usage as a phenolic raw material for the manufacture of certain resins and plastics due to its unusual electrical and frictional properties [3]. Chemical and physical modes of nanoparticle synthesis aimed at

Palanivel Velmurugan and Mahudunan Iydroose made equal contributions to this work.

P. Velmurugan · S.-M. Lee · M. Cho · J.-H. Park · B.-T. Oh (✉)
Division of Biotechnology Advanced Institute of Environment and Bioscience, College of Environmental and Bioresource Sciences, Chonbuk National University, Iksan, Jeonbuk 570-752, South Korea
e-mail: btoh@jbnu.ac.kr

P. Velmurugan
e-mail: palanivelmurugan2008@gmail.com

M. Iydroose
Department of Environmental Sciences, Bharathiar University, Coimbatore 641-046, Tamil Nadu, India

V. Balachandar
Division of Human Genetics, Department of Zoology, Bharathiar University, Coimbatore 641-046, Tamil Nadu, India

controlling the physical properties of the particles are currently employed in the production of metal nanoparticles [4]. Earlier report has shown some agro-industrial residues have the capacity to produce nanoparticles [5]. Nanoparticles have attracted considerable attention in recent years because they have diverse applications [6, 7]. In this study, we describe the synthesis and characterization of silver (Ag NPs) and gold (Au NPs) nanoparticles using CNSL obtained from the cashew nut separation process. In summation, the antibacterial activity of the Ag and Au NPs against fish pathogens was evaluated.

## Materials and Methods

### CSNL Preparation

The shells (50 g) of cashew nuts (*Anacardium occidentale*) procured from a cashew nut separating plant (Panruti, Tamilnadu, India) were washed thoroughly dried and ground using a stone grinder. Twenty grams of cashew nut shell were boiled in a 500 mL beaker, using 250 mL of Milli-Q Ultrapure water, for 15 min at 100 °C. The beaker was covered with aluminum foil in order to prevent excess evaporation. The contents of the beaker were cooled, mixed thoroughly and filtered through Whatman No. 1 filter paper to obtain the extract. This extract was prepared freshly for each experiment.

### Syntheses of Silver and Gold Nanoparticles

Silver nitrate ($AgNO_3$) acquired from DaeJung Chemicals, South Korea, and chloroauric acid ($HAuCl_4$) from Kojima Chemicals, South Korea, was used for the synthesis of Ag and Au NPs, respectively. In 100-mL Erlenmeyer flasks, 45 mL of Milli-Q Ultrapure water and 5 mL of CNSL was added to separate Ag and Au NPs. Combination of nanoparticle was performed by the addition of 1 mM $AgNO_3$ for silver and 1 mM $HAuCl_4$ for gold into the reaction mixture (water and CSNL extract).

### Isolation of Silver and Gold Nanoparticles

After conformation of the nanoparticles formations. The reaction mixture was filtered through 0.22-μm Steritop Millipore filters and centrifuged at 12,000 rpm for 15 min for Ag and Au NPs isolation. The obtained NPs were freeze-dried to obtain a powder.

### Characterization of Silver and Gold Nanoparticles

The Ag and Au NPs were confirmed by scanning the absorption maximum of the reaction mixtures between 200 and 800 nm on a UV-1800 UV–VIS spectrophotometer (Shimadzu, Japan).Scanning electron microscopy with energy dispersive spectroscopy (SEM-EDS, JEOL-64000, Japan) analysis confirmed the formation of Ag and Au NPs. The morphologies, and size distributions of Ag and Au NPs were analyzed using transmission electron microscopy (TEM, Hitachi, H-n650, Japan). X-ray diffraction (XRD) measurements of Ag NPs and Au NPs were analyzed on a drop-coated glass substrate in a Rigaku instrument, Japan. FT-IR spectra of Ag and Au NPs were obtained with a Perkin-Elmer Fourier transform infrared spectroscopy (FTIR) spectrophotometer (Norwalk, USA) in the diffuse reflectance mode at a resolution of 4 particles $cm^{-1}$ in KBr pellets.

### Antibacterial Assay

#### *Bacterial Strains*

*Aeromonas hydrophila-MTCC 646, Aeromonas bestiarum-MTCC 10106, Pseudomonas fluorescens-MTCC 67,* and *Edwardsiella tarda-MTCC 2400* acquired from microbial type culture collection (MTCC) Chandigarh, India was used as test strains. Strains were maintained and grown on nutrient agar.

#### *Agar Well Diffusion Assay*

The well diffusion method was used to study the antibacterial activity of the synthesized Ag and Au NPs [8]. The bacterial suspensions were prepared by growing a single colony overnight in Luria–Bertani broth and by adjusting the turbidity to 0.5 McFarland standards [8, 9]. Mueller–Hinton agar plates were inoculated with each bacterial suspension and 0.1 mg of the Ag and Au NPs were dissolved in 1 mL deionized water separately. Approximately 50 μL of the resulting solution was added to the center of well with a diameter of 8 mm. Control plates were made using wells containing CSNL only. Tetra-cycline was used as a positive control. The plates were incubated at 37 °C for 24 h in a bacteriological incubator, and the zone of inhibition (ZoI) was measured.

#### *Minimal Inhibitory Concentration/Minimum Bactericidal Concentrations*

The minimal inhibitory concentrations (MIC) and minimum bactericidal concentration (MBC) of the Ag and Au NPs were determined by applying the MTT assay by using a 96-well microtiter plate [9]. The 5 mL of Luria–Bertani broth medium containing 10–100 μg/mL of Ag and Au NPs were prepared with single dilution. For the determination of MIC, suspending a single isolate from the Luria–

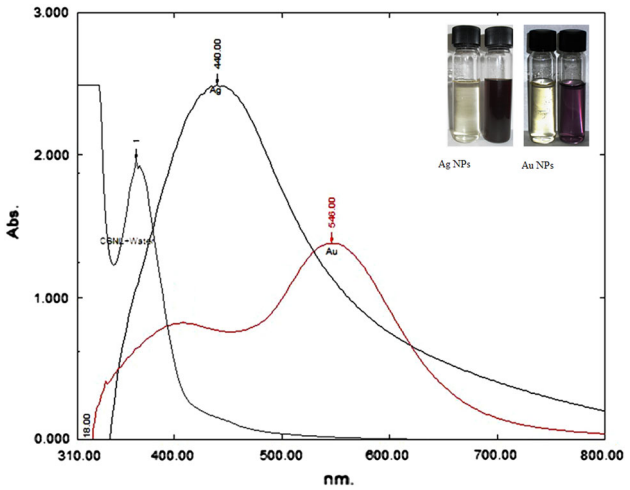


**Fig. 1** *Inset* show the formation of Ag and Au NPs

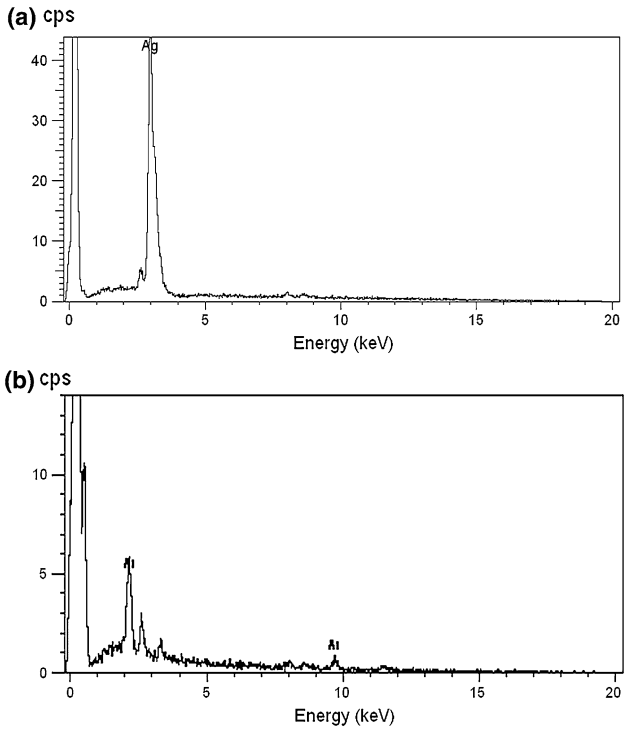


**Fig. 2** SEM-EDS spectra of **a** silver and **b** gold nanoparticles synthesized using CSNL

Bertani agar plates and inoculates into 50 µL of Luria–Bertani broth. After 24 h of incubation, suspensions were diluted in Milli-Q Ultrapure water to obtain final inoculums of $5 \times 10^5$–$5 \times 10^6$ colony-forming units/mL. Purity examination of the isolates were checked by Gram staining and colony morphology during the study. Twofold serial dilutions of Ag and Au NPs solutions were prepared in Luria–Bertani broth in 98-well plates starting from a stock solution of $10^{-2}$ M. Microtiter plate containing 0.05 mL of the serial compound dilutions was filled with an equal volume of each bacterial inoculum. After incubation for 18–24 h at 35 °C, MIC was determined with polar star optima micro plate reader (BMG LABTECH GmbH, Germany). The absorbance was compared with the negative control wells are determined, broth with Ag and Au NPs or broth alone and without inoculum with the lowest concentration of the compound [10, 11]. The mean values of three independent replicates were expressed in results.

### Statistical Analysis

Each experiment was finished in triplicates, and the resulting bacterial growths on replicates were reported in corresponding to a particular sample in the mean ± standard deviation (n = 3). The experimental analysis was based on three independent sample analyses for MIC and MBC.

## Results

### Syntheses, Characterizations and Morphology of Ag and Au Nanoparticles

The additions of 1 mM each of $AgNO_3$ and $HAuCl_4$ to the respective reaction mixtures resulted in solutions with a yellowish brown color and a dark purple color, indicating the formations of Ag and Au NPs, respectively (Fig. 1). The color developments may be explained by the excitation of surface plasmon vibrations in the metal nanoparticles [10, 11]. The silver surface plasmon resonance (SPR) band occurred at 440 nm, and the intensity steadily increased as a function of time, without any shift in the peak wavelength (Fig. 1) [11, 12]. In the gold ion reduction, the SPR band occurred at 546 nm (Fig. 1) [12, 13]. The EDS of the NPs synthesized after treatment with CNSL and 1 mM of either silver $AgNO_3$ or $HAuCl_4$ solution are shown in Fig. 2a, b, which illustrate the presence of Ag and Au NPs. Review shows different characterizations of Ag and Au NPs using EDS [12–14]. The energy-dispersive spectroscopy analysis of the X-rays (EDS; Fig. 2a, b) shows the presence of elemental silver and gold in the freeze-dried powder. These results agree with other studies on Ag and Au NPs preparation using biomaterial such as plant extracts and microorganisms reported by Shahverdi et al. [14]; Song and Kim [15]; Twu et al. [16]. The XRD patterns recorded for Au and Ag NPs show six intense peaks for silver and eight intense peaks for gold over the whole spectrum of 2θ, with values ranging from 10 to 90 (Fig. 3a, b). Intense peaks of 111, 200, 220, and 311 nanoparticles were observed, indexed as the crystalline silver and gold face-centered cubic phase. The intensity of the Bragg reflections suggests

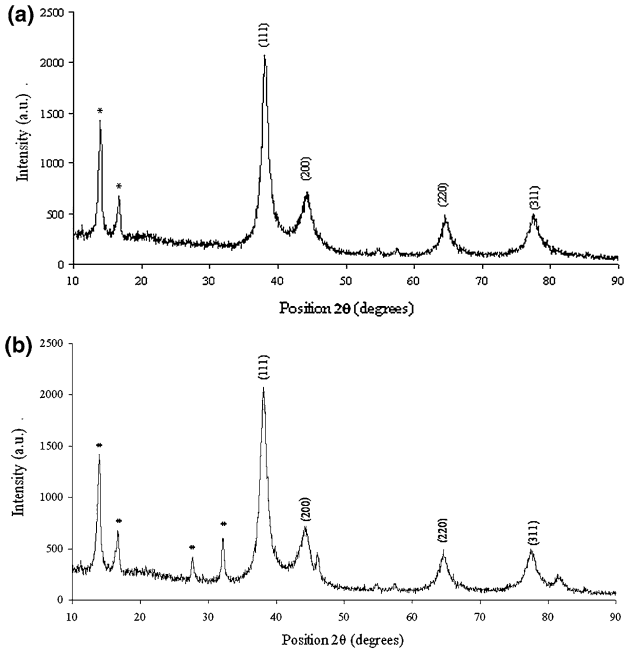


**Fig. 3** XRD patterns of **a** silver and **b** gold nanoparticles synthesized using CSNL

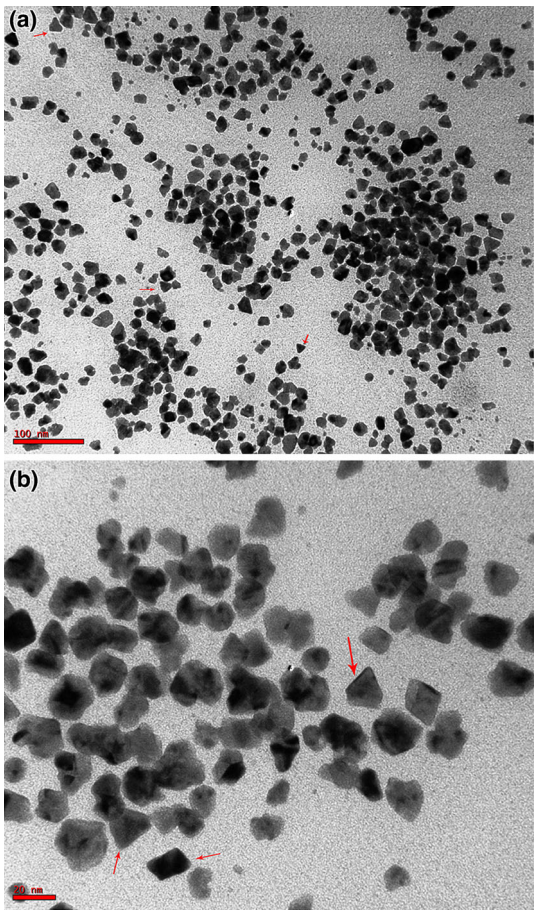


**Fig. 4** TEM micrographs of Ag NPs [*scale bar* at 100 nm (**a**) and 20 nm (**b**)] synthesized using CSNL

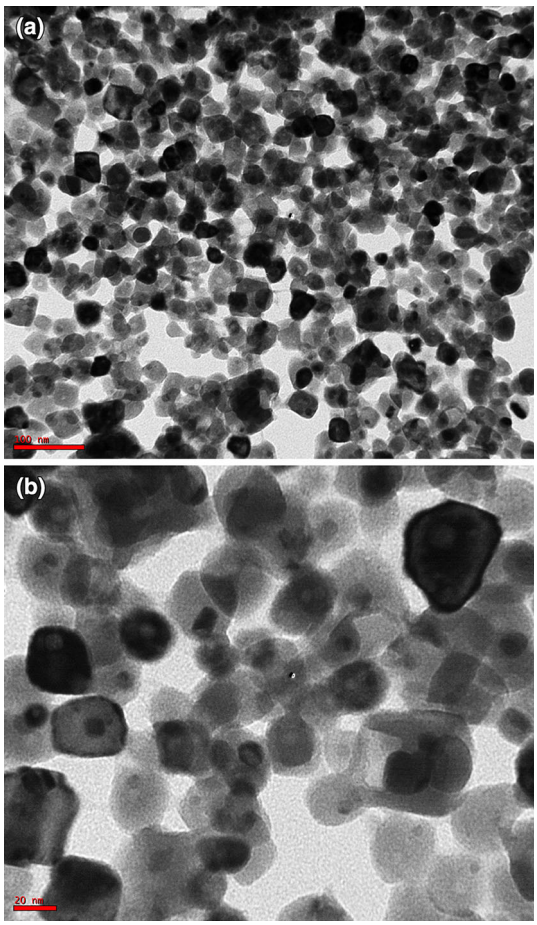


**Fig. 5** TEM micrographs of the Au NPs [*scale bar* at 100 nm (**a**) and 20 nm (**b**)] synthesized using CSNL

that there are strong X-ray scattering centers in the crystalline phase that could possibly arise from inorganic compounds present in the nanoparticles during synthesis [16, 17]. Further, the morphologies and sizes of the nanoparticles were determined with the help of TEM. The average size range of the Ag and Au NPs was 5–50 nm, as illustrated in Figs. 4a, b, 5a, b, respectively. The TEM images indicate that the Ag NPs are spherical in shape and that the Au NPs showed multiple morphologies, including spherical, triangle, truncated triangles, and decahedral morphologies with relatively uniform diameters. Figure 6a shows FT-IR spectra of the Ag NPs. Spectra obtained from the NPs manifested absorption peaks positioned at about 790.1, 1000.10, 1610.2, 2350.5, and 3400.6 in the region of 5000–4000 $cm^{-1}$. The FT-IR spectra revealed the presence of different acids and functional groups, such as anacardic acid, carboxylic acids, cardanol, cardol, 2-methylcardolketones, aldehydes, aromatic and hydroxyl functional groups in alcohols and phenolic compounds (3400.6 $cm^{-1}$), and amino acid residues present in the CSNL. These groups may lie between those of inorganic molecules and synthesized Ag NPs, which gives rise to the

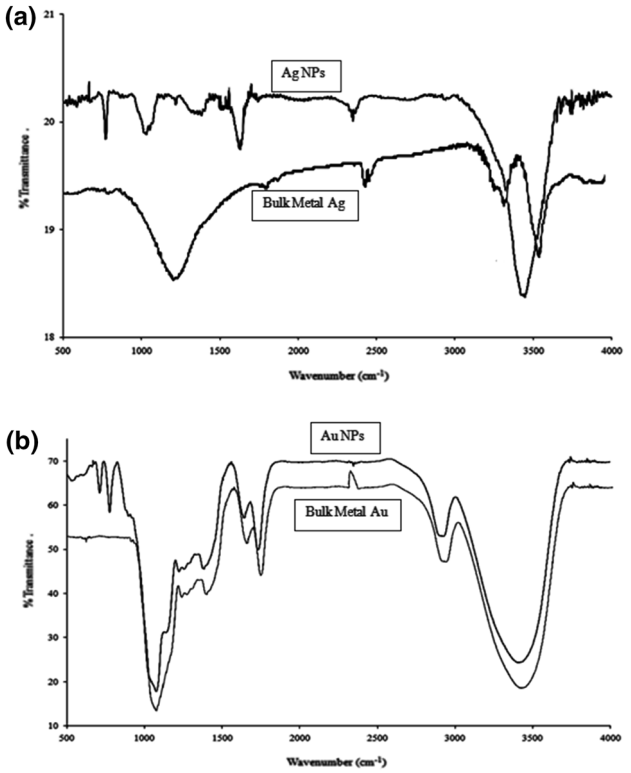


**Fig. 6** FT-IR spectra of silver (**a**) and gold (**b**) NPs synthesized using CSNL

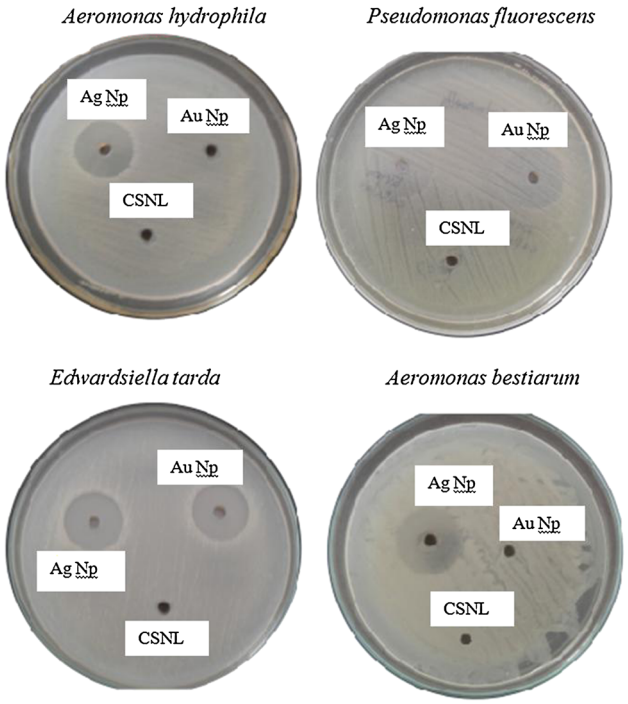


**Fig. 7** Plates showing the inhibition zones around wells for *Aeromonas hydrophila, Aeromonas bestiarum*, *Pseudomonas fluorescens,* and *Edwardsiella tarda*

well-known signatures in the infrared region of the electromagnetic spectrum [17, 18].

Our results corroborate the reports of Kaliswaralal et al. [18] the component present in CSNL can bind to nanoparticles through either free amine groups or aldehydes, aromatic, hydroxyl functional groups in alcohols, and phenolic compounds in the CSNL. With the case of Au NPs, strong bands at 1090.2, 1400.8, 1610.2, 1720.2, 2900.6, and 3400.6 $cm^{-1}$ were observed, and some weak bands at 710.2 and 790.1 $cm^{-1}$ were also recorded (Fig. 6b). The bands at 790.1, 1610.2, 1090.2, and 3400.6 $cm^{-1}$ were similar to those of the Ag NP peaks; consequently, they were attributed to the same compounds and amino acid residues. Residual peaks at 1400.8, 1720.2, and 2900.6 $cm^{-1}$ might represent the carbonyls of ketones, ester –NH stretching of the amide (II) band, carbonyl groups, or secondary amines [11, 16].

Surface plasmon resonance spectra for Ag and Au NPs were obtained at 440 and 546 nm with brown-yellow and purple color, respectively. Ag and Au NPs have free electrons, which cause an (SPR) absorption band arising from interband transitions due to the combined vibration of electrons of metal nanoparticles in resonance with the light wave [12, 13]. In this study, Ag and Au NPs are found to have (SPR) absorption bands centered at 440 and 546 nm, respectively, as shown in Fig. 1.

### *Antibacterial Activity*

The antibacterial activity of the synthesized Ag and Au NPs was tested against the Gram-negative fish pathogenic bacteria *A. hydrophila, A. bestiarum, P. fluorescens, and E. tarda*. The results of the antibacterial activity of Ag and Au NPs against fish pathogens are observed after 24 h of incubation at 37 °C was presented in Fig. 7 and Table 1. The negative control CSNL (10 mg/mL) has no remarkable interests on zone formation. Ag NPs are effective in inhibiting all the above said bacterial strains, however for Au NPs only arresting the growth of *A. bestiarum* and *P. fluorescens*. The ZOI of around 15.3 ± 0.3 (Ag NPs) was observed for *E. tarda,* 14.8 ± 0.4 *P. fluorescens,* 14.1 ± 0.6 *A. bestiarum* and 12.5 ± 0.2 for *A. hydrophila*. However in the case of Au NPs the ZOI of around 12.6 ± 0.4 and 11.2 ± 0.9 for *A. bestiarum* and *P. fluorescens,* respectively.

### *Minimal Inhibitory Concentration/Minimal Bactericidal Concentration*

The MIC was determined as the lowest concentration at which no visible growth of the fish pathogen was observed. The MIC of Ag NPs were found to be 124 ± 9.1 μg/mL for *E. tarda,* 180 ± 14.6 μg/mL, *P. fluorescens,* 312 ± 9.4 μg/mL, *A. bestiarum,* and 250 ± 10.2 μg/mL, *A. hydrophila,*

**Table 1** Antibacterial activity of CSNL mediated synthesized Ag and Au nanoparticles (ZOI, MIC and MBC) against *Aeromonas hydrophila*, *Aeromonas bestiarum*, *Pseudomonas fluorescens*, and *Edwardsiella tarda* fish pathogens

| Bacterial strains | Gram class | ZOI (mm) | MIC (μg/mL) | MBC (μg/mL) | Control positive TC (mm) |
|---|---|---|---|---|---|
| Silver nanoparticle | | | | | |
| *Aeromonas hydrophila* | Gram-negative, rod-shaped | 12.5 ± 0.2 | 250 ± 10.2 | 322 ± 9.2 | 21.1 ± 0.3 |
| *Aeromonas bestiarum* | Gram-negative, rod-shaped | 14.1 ± 0.6 | 312 ± 9.4 | 205 ± 10.5 | 20.4 ± 0.3 |
| *Pseudomonas fluorescens* | Gram-negative, rod-shaped | 14.8 ± 0.4 | 180 ± 14.6 | 183 ± 14.6 | 23.1 ± 0.1 |
| *Edwardsiella tarda* | Gram-negative, straight rod-shaped | 15.3 ± 0.3 | 124 ± 9.1 | 128 ± 11.0 | 16.4 ± 0.2 |
| Gold nanoparticle | | | | | |
| *Aeromonas hydrophila* | Gram-negative, rod-shaped | NZ | – | – | 21.1 ± 0.3 |
| *Aeromonas bestiarum* | Gram-negative, rod-shaped | 12.6 ± 0.4 | 294 ± 12.8 | 294 ± 9.4 | 20.4 ± 0.3 |
| *Pseudomonas fluorescens* | Gram-negative, rod-shaped | 11.2 ± 0.9 | 386 ± 12.7 | 363 ± 16.2 | 23.1 ± 0.1 |
| *Edwardsiella tarda* | Gram-negative, straight rod-shaped | NZ | – | – | 16.4 ± 0.2 |

Mean ± standard deviation was used to expressed the values as (n = 3). 10–100 μg/mL concentration of Ag and Au nanoparticles was used

*Ag* silver, *Au* gold, *ZOI* zone of inhibition, *MIC* minimum inhibitory concentration, *MBC* minimum bactericidal concentration, *CSNL* cashew nut shell liquid, *TC* tetracycline, *NZ* no zone

respectively and for Au NPs found to be 294 ± 12.8 μg/mL *A. bestiarum* and 386 ± 12.7 μg/mL for *P. fluorescens* respectively (Table 1). The MBC values for Au NPs is about 128 ± 11.0 μg/mL for *E. tarda,* 183 ± 14.6 μg/mL *P. fluorescens,* 205 ± 10.5 μg/mL *A. bestiarum*, and 322 ± 9.2 μg/mL *A. hydrophila.* For Au NP the MBC was 363 ± 16.2 μg/mL *P. fluorescens* and 294 ± 9.42 μg/mL *A. bestiarum*, respectively (Table 1).

## Discussion

This study evaluated the efficacy of the inhibitory effect of Ag and Au NPs synthesized using CSNL against bacterial fish pathogens. Especially with regards to those that cause important disease outbreaks in the aquaculture industry that have severe economic impacts [19]. Therefore, emerging nanoparticle antimicrobial therapies are of great interest ecological conservations. Through various instrumental analysis, it shows that CSNL has the capacity to produce various morphology of Ag and Au NPs. This present study concluded that synthesized Au NPs has maximum inhibitory effect against all the bacterial strains used. However, Au NPs had less effect on *P. fluorescens* and *A. bestiarum*. In application point of view Au NPs are not suitable, due to its economical value when compare to Ag NPs. The bacterial growth inhibition around the well is due to incorporation of metallic silver particles, which supports is to obtain high specific surface area and a high fraction of surface atoms of NPs will lead to high bactericide activity [8]. The differential sensitivity of bacteria towards Ag and Au NPs depends upon size of particles, route of synthesis, structure of bacterial cell wall, and the mode of contact with organisms with nanoparticles [11, 20]. The difference in activity against these two nanoparticles could be attributed to the compound present in the metals and the size of nanoparticles obtained might be a reason to high/low antibacterial activity. A recent study describes, when irradiation applied at 4 kGy without Ag NPs and at 2 kGy with Ag NPs against total aerobic mesophilic bacteria, Enterobacteriaceae, *Escherichia coli* and *Clostridium perfringens* shows greater inhibition zones in antimicrobial treatments of the packaging films using Ag NPs impregnation and gamma irradiation [20–22]. The CSNL mediated synthesized Ag and Au NPs with bactericidal activity might became an alternative to antibiotics used in fishery and aquaculture industry [22–24]. In the fact of controlling chemical toxicity in the environment, occurred through the antibiotic used in aquaculture industry can be replaced by eco-friendly biosynthesized Ag NPs [25].

**Acknowledgments** This research was supported by Korean National Research Foundation (Korean Ministry of Education, Science and Technology, Award NRF-2011-35B-D00020).

## References

1. Mitchell JD, Mori SA (1987) The cashew and its relatives (Anacardium: Anacardiaceae). Mem N Y Bot Gard 42:1–76
2. Santos ML, Magalhães GC (1999) Utilization of cashew nut shell liquid from *Anacardium Occidentale* as starting material for organic synthesis: a novel route to lasiodiplodin from cardols. J Braz Chem Soc 10:13–20
3. John HPT, Naina V (1997) Synthesis of saturated anacardic acids, and alkenyl and alkynyl analogues. J Chem Res (S) 9:14–15
4. Brust M, Kiely CJ (2002) Some recent advances in nanostructure preparation from gold and silver particles: a short topical review. Colloids Surf A Physicochem Eng Asp 202:175–186
5. Bankar A, Joshi B, Kumar AR, Zinjarde S (2010) Banana peel extract mediated synthesis of gold nanoparticles. Colloids Surf B: Biointerfaces 80:45–50

6. Mohanpuria P, Rana NK, Yadav SK (2008) Biosynthesis of nanoparticles: technological concepts and future applications. J Nanopart Res 10:507–517
7. Kumar V, Yadav SK (2009) Plant-mediated synthesis of silver and gold nanoparticles and their applications. J Chem Technol Biotechnol 84:151–157
8. Kora AJ, Sashidhar RB, Arunachalam J (2010) Gum kondagogu (*Cochlospermum gossypium*): a template for the green synthesis and stabilization of silver nanoparticles with antibacterial application. J Carbohydr Polym 82:670–679
9. Krishnaraj C, Jagan EG, Rajasekar S, Selvakumar P, Kalaichelvan PT, Mohan N (2010) Synthesis of silver nanoparticles using *Acalypha indica* leaf extracts and its antibacterial activity against water borne pathogens. Colloid Surf B 76:50–56
10. Wiegand I, Hilpert K, Hancock RE (2008) Agar and broth dilution methods to determine the minimal inhibitory concentration (MIC) of antimicrobial substances. Nat Protoc 3:163–175
11. Vellora V, Padil T, Cerník M (2013) Green synthesis of copper oxide nanoparticles using gum karaya as a biotemplate and their antibacterial application. Int J Nanomed 8:889–898
12. Dubey SP, Lahtinen M, Sillanpaa M (2010) Green synthesis and characterizations of silver and gold nanoparticles using leaf extract of *Rosa rugosa*. Colloids Surf A Physicochem Eng Asp 364:34–41
13. Badri Narayanan K, Sakthivel N (2008) Coriander leaf mediated biosynthesis of gold nanoparticles. Mater Lett 62:4588–4590
14. Shahverdi AR, Minaeian S, Shahverdi HR, Jamalifar H, Nohi AA (2007) Rapid synthesis of silver nanoparticles using culture supernatants of *Enterobacteria*: a novel biological approach. Process Biochem 42:919–923
15. Song JY, Kim BS (2008) Biological synthesis of bimetallic Au/Ag nanoparticles using persimmon (*Diopyros kaki*) leaf extract. Korean J Chem Eng 25:808–811
16. Twu YK, Chen YW, Shih CM (2008) Preparation of silver nanoparticles using chitosan suspensions. Powder Technol 185: 251–257
17. Shankar SS, Rai A, Ahmad A, Sastry M (2004) Rapid synthesis of Au, Ag and bimetallic Au core-Ag shell nanoparticles using neem (*Azadirachta indica)* leaf broth. J Colloid Interface Sci 275:496–502
18. Kalishwaralal K, Deepak V, Ram Kumar Pandian SB, Kottaisamy M, BarathmaniKanth S, Kartikeyan B, Gurunathan S (2010) Biosynthesis of silver and gold nanoparticles using *Brevibacterium casei*. Colloids Surf B Biointerfaces 77:257–262
19. Paramashivappa R, Kumar PP, Vithayathil PJ, Rao AS (2001) Novel method for isolation of all major phenolic constituents from cashew (*Anacardium occidentale* L.) nut shell liquid. J Agric Food Chem 49:2548–2551
20. Philip D (2008) Synthesis and spectroscopic characterization of gold nanoparticles. Spectrochim Acta A Mol Biomol Spectrosc 71:80–85
21. Liang X, Sun M, Li L, Qiao R, Chen K, Xiao Q, Xu F (2012) Preparation and antibacterial activities of polyaniline/$Cu_{0.05}Zn_{0.95}O$ nanocomposites. Dalton Trans 41:2804–2811
22. Singh M, Kumar P, Patel SKS (2013) Production of polyhydroxyalkanoate co-polymer by *Bacillus thuringiensis*. Indian J Microbiol 53:77–83
23. Das BK, Samal SK, Samantaray BR, Sethi S, Pattnaik P, Mishra BK (2006) Antagonistic activity of cellular components of *Pseudomonas* species against *Aeromonas hydrophila.* Aquaculture 253:17–24
24. Mahanty A, Mishra S, Bosu R, Maurya UK, Netam SP, Sarkar B (2013) Phytoextracts-synthesized silver nanoparticles inhibit bacterial fish pathogen *Aeromonas hydrophila*. Indian J Microbiol 53:438–446
25. Odeyemi OA, Asmat A, Usup G (2012) Antibiotics resistance and putative virulence factors of *Aeromonas hydrophila* isolated from estuary. J Microbiol Biotechnol Food Sci 1:1339–1357